

CHAPTER 128

A NUMERICAL MODEL FOR THE HYDROMECHANICS OF LAGOONS

J. van de KREEKE¹

ABSTRACT

A numerical model is presented to describe the hydromechanics of lagoons connected to the ocean by relatively narrow inlets. Because special attention is given to the flushing, all second order terms in the hydrodynamic equations are retained. The study is restricted to lagoons with a one-dimensional flow pattern and water of uniform density. In designing a numerical solution to the equations, the inlet equations are regarded as implicit boundary conditions to the equations describing the flow in the lagoon proper. The advantages of this approach are: (1) the size of the computational grid in the lagoon can be chosen independently of the relatively small dimensions of the inlets and (2) the flow at branching inlets (an inlet connecting a lagoon to the ocean such that branching of the inlet flow can occur) still can be described by a one-dimensional tidal model.

The predictive capability of the numerical model is confirmed by favorable comparison between measured and computed particle paths and net transport for a series of laboratory experiments. In the experiments a canal of uniform width and depth is freely connected to a tidal basin at one end and at the other end is connected to the same basin by a submerged weir.

INTRODUCTION

The computational model presented in this paper is designed to simulate the tidal motion in the inland coastal waters found along the Florida Atlantic coast and the Gulf of Mexico coast. Many of these waters, from now on designated as lagoons, are characterized by (1) an elongated shape, (2) narrow inlets connecting the actual lagoon to the ocean and (3) fairly large tidal amplitude to depth ratios. The elongated shape of the lagoons permits the use of the one-dimensional tidal equations. Because of (3), the non-linear terms in the equations are retained. Also, these terms must be accounted for to correctly reproduce the tide-induced flushing.

The numerical scheme for the lagoon proper is based on an explicit difference scheme described by Reid and Bodine [3]. The inlets are incorporated in the model using Dronkers [2] work on river junctions and the computational scheme presented by Balloffet [1]. The performance of the numerical model is evaluated by comparing computed and measured results for a series of laboratory experiments.

¹Assistant Professor, Division of Ocean Engineering, Rosenstiel School of Marine and Atmospheric Science, University of Miami

NUMERICAL MODEL

Equations

The equations used to describe the flow in the lagoon are the equation of continuity

$$\frac{\partial \eta}{\partial t} + \frac{\partial q}{\partial x} = M \quad (1)$$

in which η = water surface elevation, q = discharge per unit width M = storage, t = time coordinate, x = space coordinate, and the equation of motion

$$\frac{\partial q}{\partial t} + \frac{1}{h} \frac{\partial q^2}{\partial x} + g(h + \eta) \frac{\partial \eta}{\partial x} = - \frac{Fq|q|}{(h + \eta)^2} \quad (2)$$

in which h = mean depth, g = gravitational acceleration, F = resistance coefficient. For the inlets, because of the complexity of the flow (contraction, lateral stresses), recourse is taken to a semi-empirical representation

$$Q = \pm \left(\frac{2g\bar{P}^2}{2FL + m\bar{R}} \right)^{\frac{3}{2}} \left[\frac{-}{\bar{R}} + \frac{B}{\bar{P}} \frac{(\eta_o + \eta_i)}{2} \right]^{\frac{3}{2}} \sqrt{|\eta_o - \eta_i|} \quad (3)$$

- sign for $\eta_i \leq \eta_o$

+ sign for $\eta_i \geq \eta_o$

in which Q = total discharge, \bar{P} = wetted perimeter of inlet cross section measured at mean ocean level, \bar{R} = hydraulic radius for the inlet cross section measured at mean ocean level, L = length of inlet, B = width of inlet, η_o = ocean tide, η_i = lagoon tide, m = coefficient which accounts for entrance losses and the non-uniform velocity distribution.

Numerical Scheme

The numerical scheme for the lagoon is space and time staggered. Water levels are computed at $n\Delta t$ and discharges at $(n + 1/2)\Delta t$. The water levels apply at the center of the grid blocks and the discharges are computed at the gridlines; see Figure 1. The mean depth h and the lateral inflow or rainfall are given at the time level and location of η . The basic recurrence equations for the one-dimensional tidal equations are

$$q'(i) = \frac{1}{G(i-1)} \left[q(i) + \frac{g\Delta t}{2\Delta x} (D(i) + D(i-1)) (\eta(i-1) - \eta(i)) \right] \quad (4)$$

$$\eta'(i) = \eta(i) + \frac{\Delta t}{\Delta x} (q'(i) - q'(i+1)) + M(i)\Delta t \quad (5)$$

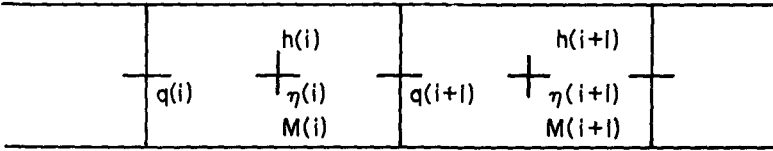


FIGURE 1. LOCATION OF VARIABLES IN THE NUMERICAL GRID

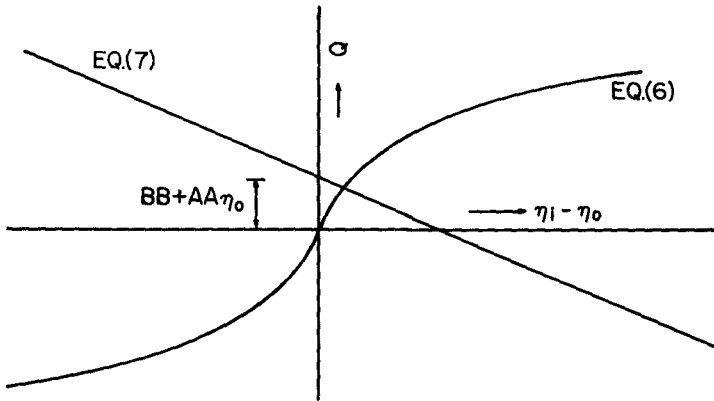


FIGURE 3. FUNCTIONS REPRESENTED BY EQUATIONS (6) AND (7)

in which

$$D(i) = \eta(i) + h(i)$$

$$G(i-1) = 1 + \frac{4F \Delta t |q(i)|}{(D(i) + D(i-1))^2} + \frac{\Delta t (q(i+1) - q(i-1))}{\Delta x (h(i) + h(i-1))}$$

Primed symbols denote values of the variables at time step Δt later. Equations (4) and (5) are based respectively upon the differential Equations (2) and (1). The differential quotients in these equations are replaced by difference quotients using central differences. The difference quotients for Equation (1) are centered about $(n + 1/2)\Delta t$ and the location of η . The difference quotients for Equation (2) are centered about time level $n.\Delta t$ and are centered in space about the location of q . Starting from the initial conditions all the q 's are computed for the next time level by means of Equation (4), then the η 's are computed using Equation (5). It is noted that because of the convective acceleration, the recurrence formula (4) includes values as far apart as 2 space steps; see expression for $G(i-1)$. This leads to difficulties when the boundary conditions at open boundaries are given as water levels. In that case, the convective acceleration is taken off center for the grids adjacent to those boundaries. After some algebraic manipulation, the following result is obtained.

$$Q = \pm DD \sqrt{|\eta_i - \eta_o|}$$

$$+ \text{sign for } \eta_i \geq \eta_o$$

$$- \text{sign for } \eta_i \leq \eta_o$$
(6)

in which

$$Q = \frac{Q'(i+1) + Q(i+1)}{2}$$

$$DD = \sqrt{\frac{2g\bar{P}^2}{2FL + m\bar{R}}} \left(\bar{R} + \frac{\bar{B}}{\bar{P}} \frac{\eta_o + \eta_i}{2} \right)^{3/2}$$

In the computational procedure the inlet equation, Equation (3), may be regarded as an implicit boundary condition for the flow in the lagoon.

The way in which this boundary condition is incorporated in the numerical scheme depends on the inlet configuration. The following two cases are considered:

- An inlet connecting a lagoon to the ocean such that no branching of the inlet flow occurs; see Figure 2A.
- An inlet connecting a lagoon to the ocean such that branching of the inlet flow can occur; see Figure 2B.

Consider the "nonbranching inlet"; see Figure 2A. The total discharge Q rather than the discharge per unit width, q , is used as a dependent variable. An auxiliary water level η_i is introduced which is computed at the same time level as the water levels in the lagoon. Starting from the initial conditions, all the discharges in the lagoon except $Q(i+1)$ can be computed using the procedure described before. The value of $Q(i+1)$ is then computed as follows. $Q(i+1)$ is related to the known ocean level η_o and the auxiliary level η_i by means of the inlet equation. A second equation relating $Q(i+1)$ and η_i is found by applying the dynamic equation, Equation (2), between the discharge stations $Q(i+1)$ and $Q(i)$. Note that when computing the flow in the lagoon, the dynamic equation is applied between two water level stations. The difference form of the dynamic equation applied between $Q(i+1)$ and $Q(i)$ yields

$$Q = AA(\eta_i - \eta_o) + BB + AA \eta_o \tag{7}$$

in which

$$Q = \frac{Q'(i+1) + Q(i+1)}{2}$$

$$AA = \frac{-g D(i) B l \Delta t}{G \Delta x}$$

$$BB = \{Q(i+1) + Q(i) - Q'(i) \cdot G + \frac{g B l D(i) \Delta t}{\Delta x}$$

$$[\eta(i) + \eta(i-1)]\} / \left[2G + \frac{Q(i+1)}{2} \right]$$

$$G = 1 + \frac{F \Delta t [Q(i+1) + Q(i)]}{2D(i)^2 B l} + \frac{2 \Delta t [Q(i+1) - Q(i)]}{\Delta x h(i) B l}$$

In determining the difference form, the terms in both the inlet and dynamic equation are centered about $n \cdot \Delta t$.

The general shapes of the curves $Q = f(\eta_i - \eta_o)$ represented by the Equations (6) and (7) are indicated in Figure 3. Equation (7) represents

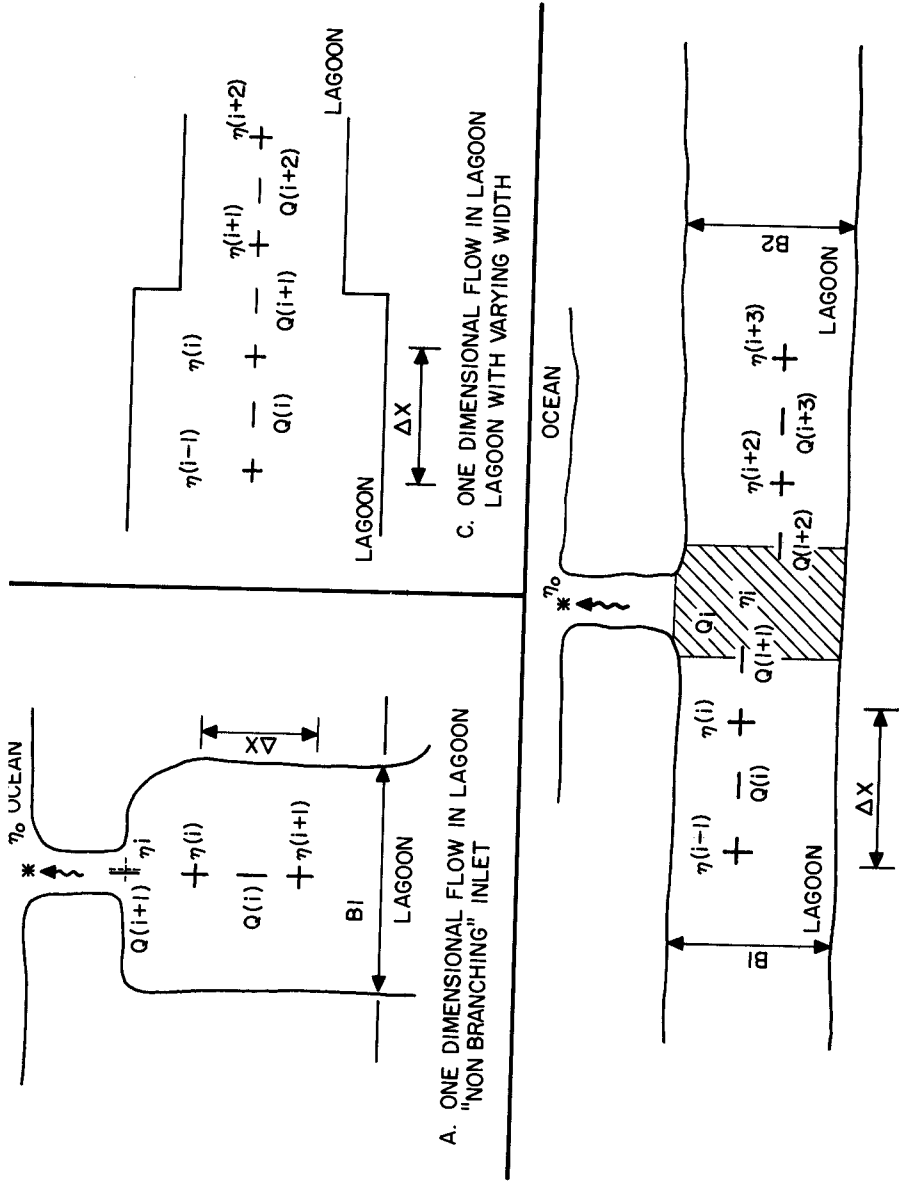


FIGURE 2. GFTD SCHEME FOR DIFFERENT INLET CONFIGURATIONS

a straight line. The slope of this line, AA, is for most practical cases negative. Therefore, the sign of $(BB + AA\eta_o)$, which is a known quantity, determines the sign of $(\eta_i - \eta_o)$ which in turn determines the sign to be used in Equation (6). Eliminating $(\eta_i - \eta_o)$ between Equations (6) and (7) yields

$$Q = \frac{1 - \sqrt{1 - 4 \frac{AA}{DD^2} (AA\eta_o + BB)}}{2 \frac{AA}{DD^2}} \quad (8)$$

for $(BB + AA\eta_o) \geq 0$

and

$$Q = \frac{1 - \sqrt{1 + 4 \frac{AA}{DD^2} (AA\eta_o + BB)}}{-2 \frac{AA}{DD^2}} \quad (9)$$

for $(BB + AA\eta_o) \leq 0$.

Note that only the first order terms in $(\eta_i - \eta_o)$ are eliminated because second order terms are still present in the factor DD. Equations (8) and (9) therefore may be regarded as being quasi-linear, which suggests finding a solution by means of a perturbation method. First the value of $(\eta_i - \eta_o)$ in DD is taken equal to the value at the previous time step. The value of Q can then be found from Equation (8) or (9) depending on the sign of $(BB + AA\eta_o)$. Knowing Q, the value of $(\eta_i - \eta_o)$ is determined from either Equations(6) or (7). This value of $(\eta_i - \eta_o)$ is substituted in DD. The Procedure then is repeated until the difference between the computed and previously computed value of Q is within certain limits.

The numerical scheme for the "branching inlet" (see Figure 2B) involves four unknowns $Q'(i+1)$, $Q'(i+2)$, $Q'(i+2)$, Q'_i and η_i as compared to only two, $Q(i+1)$ and η_i , for the "nonbranching inlet". The four unknowns are related by the following four equations

- the inlet equation which takes the form of Equation (6) with $Q = \frac{Q'_i + Q_i}{2}$
- the dynamic equation applied between the locations of $Q(i)$ and $Q(i+1)$; this equation takes the form of Equation (7).
- the dynamic equation applied between the locations of $Q(i+2)$ and $Q(i+3)$; this equation takes the form of Equation (7) with

$Q(i)$ replaced by $Q(i+3)$, $Q(i+1)$ replaced by $Q(i+2)$, $\eta(i)$ replaced by $\eta(i+2)$, $\eta(i-1)$ replaced by $\eta(i+3)$, $h(i)$ replaced by $h(i+2)$, Δx replaced by $-\Delta x$, and $B1$ replaced by $B2$.

the continuity condition which, when assuming that the water level in the hatched area is the same everywhere, takes the form

$$Q(i+1) = Q_1 + Q(i+2)$$

Elimination of $Q(i+1)$ and $Q(i+2)$ between the two dynamic equations and the continuity equation yields a relation between Q_1 and η_1 similar to Equation (7). This equation together with the inlet equation then can be solved following the procedure described before.

Finally, it is noted that in one-dimensional flow computations, it is often necessary to divide the lagoon into parts with different widths; see Figure 2C. The flow at the boundary of two such parts may be computed following a procedure similar to the one applied to the "nonbranching inlet", replacing the inlet equation by a second dynamic equation between the locations of $Q(i+1)$ and $Q(i+2)$.

COMPARISON WITH LABORATORY EXPERIMENTS

To evaluate the capability of the computational model to predict the water motion in lagoons, computed and measured float paths were compared for a series of laboratory experiments. A straight canal of uniform depth and width simulating a lagoon, was constructed in a tidal basin; see Figure 4. The canal was open at one end and at the other end provided with a submerged sharp crested weir. The average water depths used in the experiments were 5 cm and 6.5 cm, the wave amplitudes varied between 0.7 cm and 1.2 cm and the wave periods varied between 70 sec and 120 sec. Maximum velocities in the experiments varied between 3 cm/sec and 5 cm/sec, depending on water depth, amplitude and period. Reynolds' numbers ($Re = \frac{q}{\nu}$) were larger than 800 (the limit for fully turbulent flow) 60% - 80% of the time (the exact percentage depending on depth, period and amplitude).

The floats used in the experiments were cylindrical and had a diameter of approximately 0.5 cm, the top was given a conical shape to minimize effects of surface tension. The length of the floats was chosen as large as possible to arrive at an average over depth particle path, but short enough that the float did not contact the bottom. Floats were released one at a time either in the middle of the lagoon or 5 cm from the side walls. Positions of the float were marked at each slack tide for a period of at least five tidal cycles.

Typical examples of measured and computed float paths are presented in Figure 5. In the computations the flow over the weir was described by

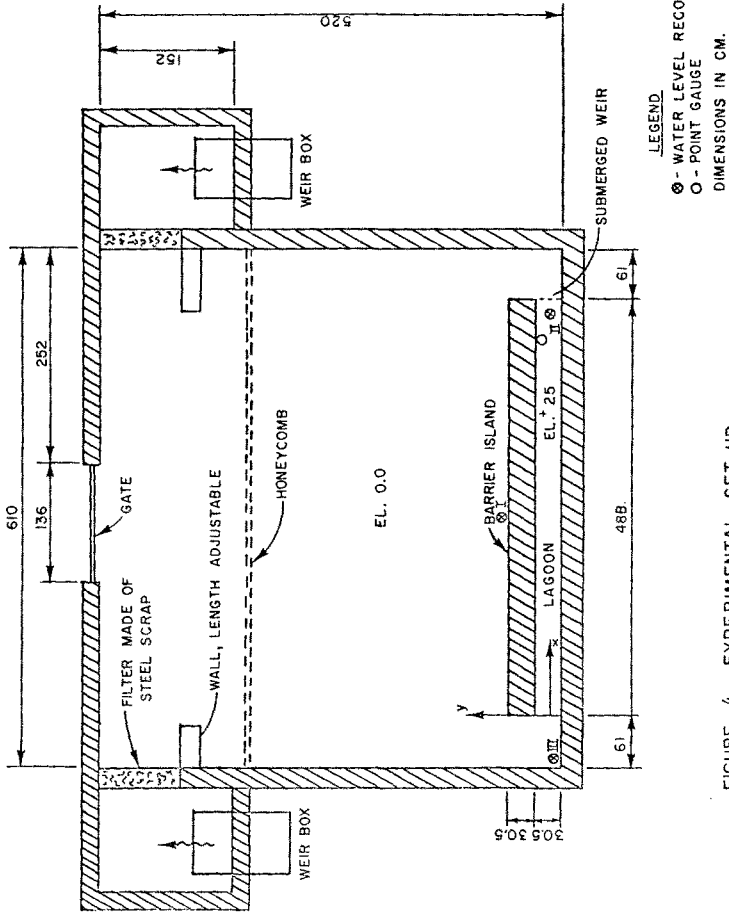


FIGURE 4 EXPERIMENTAL-SET UP

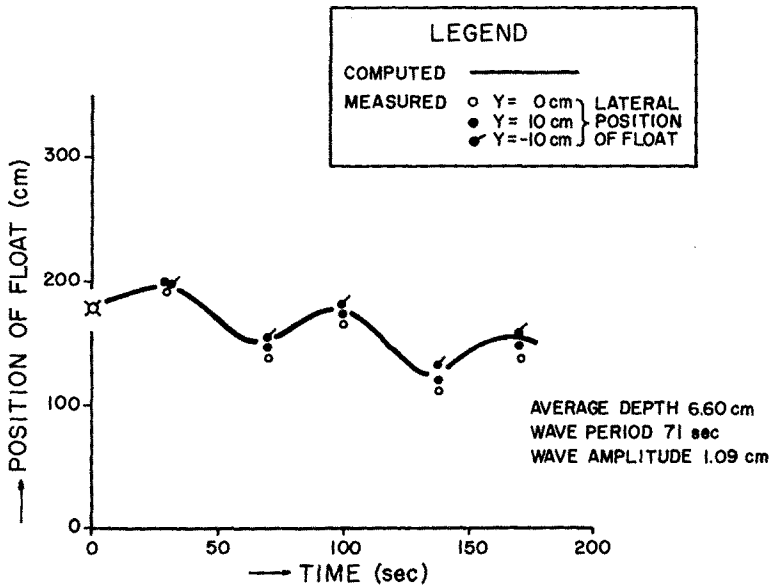
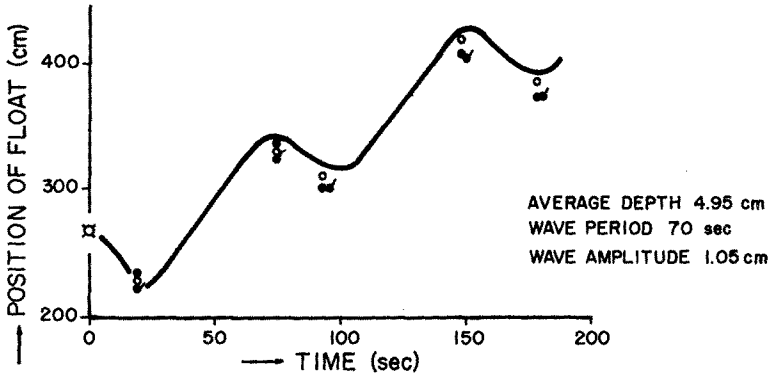


FIGURE 5. MEASURED AND COMPUTED FLOAT POSITIONS

an equation similar to Equation (3)

$$q_w = \pm \mu \pm h_w \sqrt{2g|\eta_o - \eta_i|} \quad (10)$$

+ sign for $\eta_i \geq \eta_o$

- sign for $\eta_o > \eta_i$

In Equation (10)

q_w = discharge per unit width over the weir

$\mu \pm$ = weir coefficient

h_w = total depth over weir

η_o = water level in tidal basin

η_i = water level in canal

For all the experiments the net discharge q was determined from the measured particle path using an empirical method described by van de Kreeke [4] and compared with the computed net discharge. The results are presented in Figure 6.

SUMMARY AND CONCLUSIONS

- The numerical model presented in this paper is especially designed for lagoons connected to the ocean by relatively narrow inlets and for which the flow field can be described by the one-dimensional tidal equations. The flow in the inlets is described by a semi-empirical relation. In the equations all non-linear terms are retained in order to correctly reproduce such phenomenon as tide-induced mass transport and variations in mean level along the longitudinal axis of the lagoon.
- The tidal equations are solved using an explicit difference scheme. In the computational model the inlet equations are regarded as implicit boundary conditions to the tidal equations. The advantages of this approach are: (1) the size of the computational grid in the lagoon can be chosen independently of the relatively small dimensions of the inlets and (2) the flow at branching inlets (an inlet connecting a lagoon to the ocean such that branching of the inlet flow can occur) still can be described by a one-dimensional model.
- The predictive capability of the model is confirmed by favorable comparison between measured and computed float paths and net dis-

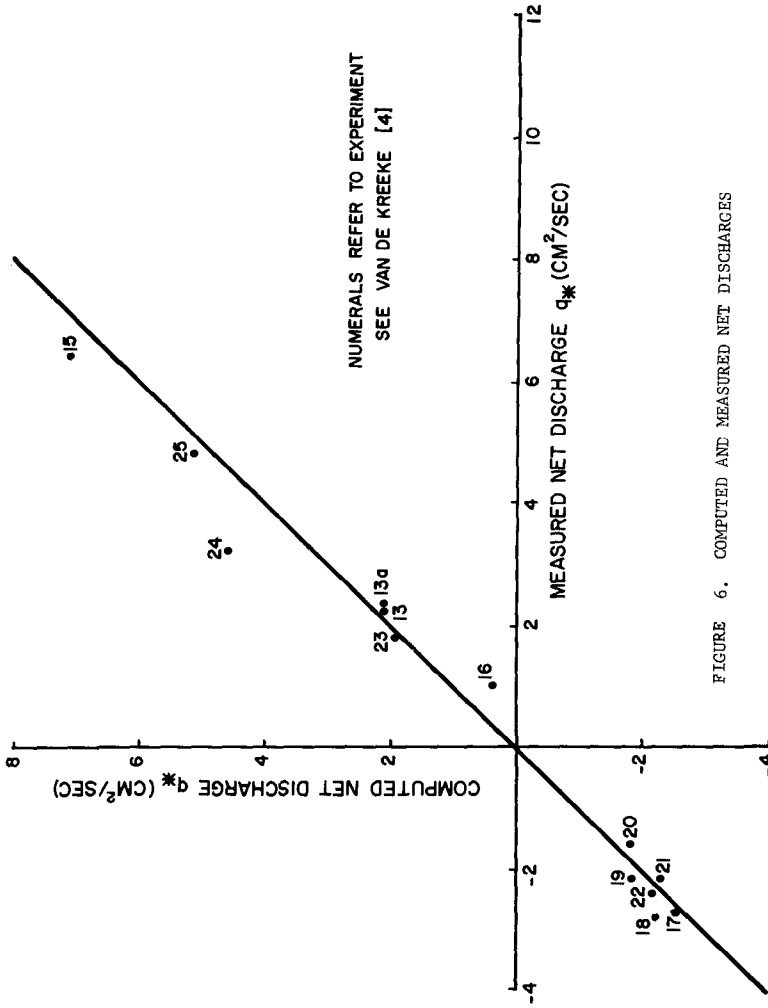


FIGURE 6. COMPUTED AND MEASURED NET DISCHARGES

charges for a series of laboratory experiments. For the experiments the relative magnitude of the different terms in the equations differs substantially from those found under prototype conditions. Therefore additional corroboration of the computational model at the prototype level is recommended.

ACKNOWLEDGEMENT

The author is indebted to R.G. Dean and B.A. Christensen for their suggestions and helpful criticism.

The study was in part supported by the Office of Water Resources Research, U.S. Department of the Interior.

REFERENCES

1. Balloffet, A., "One-Dimensional Analysis of Floods and Tides in Open Channels", Journal of the Hydraulics Division, ASCE. Vol 95, No. HY4, July 1969.
2. Dronkers, J.J. "Tidal Computations in Rivers and Coastal Waters", North-Holland Publishing Company, 1964.
3. Reid, R.O. and Bodine, B.R. "Numerical Model for Storm Surges in Galveston Bay", Journal of the Waterways and Harbors Division, ASCE, Vol. 94, No. WW1, February, 1969.
4. Van de Kreeke, "Tide-Induced Mass Transport in Shallow Lagoons", Department of Coastal and Oceanographic Engineering, University of Florida, Technical Report No. 8, October, 1971.

